Climate Change Impacts on Future Wave Climate around the UK

Bennett, William; Karunarathna, Harshinie; Mori, Nobuhito; Reeve, Dominic

Journal of *Marine Science and Engineering*

MDPI

Article

Climate Change Impacts on Future Wave Climate around the UK

William G. Bennett [1,*], Harshinie Karunarathna [1], Nobuhito Mori [2] and Dominic E. Reeve [1]

[1] Zienkiewicz Centre for Computational Engineering, College of Engineering, Bay Campus, Swansea University, Fabian Way, Swansea SA1 8EN, UK; h.u.karunarathna@swansea.ac.uk (H.K.); d.e.reeve@Swansea.ac.uk (D.E.R.)

[2] Disaster Prevention Research Institute, Uji Campus, Kyoto University, Gokasho, Uji, Kyoto 611-0011, Japan; mori@oceanwave.jp

* Correspondence: 632281@swansea.ac.uk; Tel.: +44-7734317337

Academic Editor: Dong-Sheng Jeng
Received: 28 September 2016; Accepted: 14 November 2016; Published: 18 November 2016

Abstract: Understanding the changes in future storm wave climate is crucial for coastal managers and planners to make informed decisions required for sustainable coastal management and for the renewable energy industry. To investigate potential future changes to storm climate around the UK, global wave model outputs of two time slice experiments were analysed with 1979–2009 representing present conditions and 2075–2100 representing the future climate. Three WaveNet buoy sites around the United Kingdom, which represent diverse site conditions and have long datasets, were chosen for this study. A storm event definition (Dissanayake et al., 2015) was used to separate meteorologically-independent storm events from wave data, which in turn allowed storm wave characteristics to be analysed. Model outputs were validated through a comparison of the modelled storm data with observed storm data for overlapping periods. Although no consistent trends across all future clusters were observed, there were no significant increases in storm wave height, storm count or storm power in the future, at least according to the global wave projection results provided by the chosen model.

Keywords: storm wave height; global warming; global wave modelling; wave forecasting; coastal flooding

1. Introduction

In order to develop long-term coastal defence and management strategies required for sustainable coastal management, it is important to be confident in the knowledge of any possible future changes in metocean climate. It has been recognised that there is a potential for changes both in wave climate and storm track and intensity characteristics attributed to climate change. This, together with rising sea levels may contribute to increased and altered patterns of coastal flooding and erosion in the future, as recognised by the IPCC [1]. In addition, wave climate is an important factor in offshore operations and maritime transport considering swell [2]; this highlights the importance of changes in future wave and storm climate to a wide range of both nearshore and offshore activities.

The Coordinated Ocean Wave Climate Project (COWCLIP) [3,4] supported by the Joint Technical Commission for Oceanography and Marine Meteorology World Meteorological organization (JCOMM/WMO) was developed to address the need for attention towards future changes in wave climate over the 21st Century, as well as providing a coordinated approach to global wave climate modelling, which was highlighted in the Fourth Assessment Report (AR4 [5]) and archived in the Fifth Assessment Report (AR5 [1]) by COWCLIP. The majority of the early work towards quantifying these changes only dealt with regional scale projections [6–8], with varying scope to the period and scenarios

assessed, as well as different models and domains used. Approaches have also been limited by the lack of global or large-scale future wave climate simulations, which ignore the effects of remotely-generated swell [2] and relations to general circulations (e.g., North Atlantic Oscillations: NAO). As it has been shown that swell dominates the seasonal mean significant wave height in the UK, notably in spring and summer [9], it is important to consider these effects through the use of global models.

Recently, several studies [10–12] determined current and future global wave climate using WAVEWATCH III [13] forced by a high resolution Atmospheric General Circulation Model (AGCM) developed by the Japanese Meteorological Research Institute and the Japan Meteorological Agency (MRI-JMA), in order to analyse the effect of sea surface temperature (SST) variation on wave climate in the Western North Pacific Ocean. The global wave modelling has been carried out for two time slice experiments with 1979–2009 giving the present climate and 2075–2099 providing the future climate at a 60-km resolution. The model outputs have been extensively used to investigate wave and related typhoon impacts in the North Pacific Ocean.

The present study utilises current and future wave projections [12] to analyse the implications of global climate change on storm wave climate around the UK Due to its location within the Atlantic Ocean, the UK experiences strong winds predominantly from the southwest. Autumn and winter tend to bring stronger storm systems, while spring and summer tend to experience calm swell wave conditions. In recent years, the UK has experienced a significant increase in stormy weather conditions during winter where 2013/2014 experienced a large number of storms occurring within a period of two months causing severe coastal flooding and beach erosion, which led to widespread destruction to human lives, damage to infrastructure and significant economic losses.

Since the focus here is on the UK storm wave climate, we will first derive the present (1979–2009) and future (2075–2099) storm climate in terms of the number of storms, maximum storm wave height and storm duration from the globally-predicted wave outputs. The grid of modelled wave projections around the UK is shown in Figure 1. Then, the current modelled storms will be compared with storms determined from historic wave measurements at a few locations around the UK; this will allow an investigation of the accuracy of the wave model projections around the UK Section 2 of the paper gives a description of the selected study sites. Section 3 briefly describes climate projections, the global wave modelling approach, as well as the storm definition used in this study. The modelling approach is validated in Section 4 with the model results presented in Section 5. A summary and the conclusions are given in Section 6.

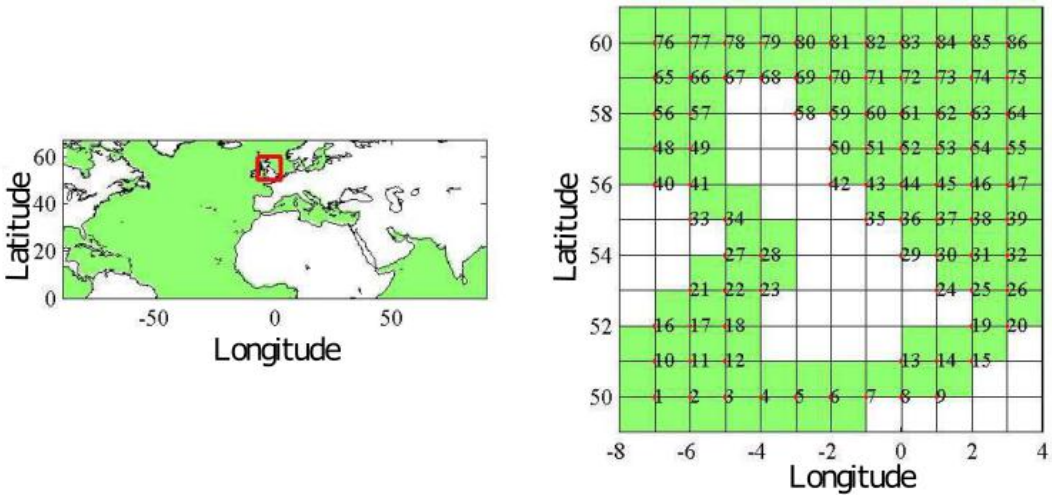

Figure 1. Wave model outputs for the UK region.

2. Study Sites around the UK

Modelled wave projections were extracted for three sites around the UK. The site locations were selected based on the availability of long-term wave measurements where waves were measured by WaveNet wave buoys operated by the Centre for Environment, Fisheries and Aquaculture Science of the UK (CEFAS). The selected sites represent diverse wave climates around the UK and contain long-term historic wave measurements that coincide with the modelled wave outputs. One site faces the North Sea, where there are less swells, but strong winter storms. On the other hand, the other site faces the Atlantic Ocean; thus, this site is influenced by large-scale atmospheric circulations and disturbances. Additionally, we select one site from a semi-enclosed sea to compare the above two different wave climate conditions excluding remote effects.

2.1. Liverpool Bay

Liverpool Bay is located within the south-eastern margin of the Irish Sea, in the UK, as shown in Figure 2. The wave climate in Liverpool Bay is mainly locally generated within the Eastern Irish Sea, with a limited fetch restricting wave development, while topographic and bathymetric features limit the incursion of Atlantic swell in to southern parts of the Irish Sea [14]. It has been found that during extreme storm conditions, significant wave heights reach 5.5 m, with a peak period less than 12 s and a mean wave period less than 8 s [15,16]. Mean significant wave height from the measured data was found to be 0.88 m, and the extreme one in 100 years wave height has been previously estimated to be 7.3 m [17].

The WaveNet Datawell Direction Waverider buoy in Liverpool Bay (Figure 2) is located approximately 17 km offshore in a 22-m water depth and has been operational since November 2002. It provides directional wave data at 30-min intervals, giving a reasonable length dataset for model validation. The overlapping period of 2002–2009 has been used in the validation of model outputs

The Sefton Coast, which forms a part of the Liverpool Bay coastline, is a 36 km-long stretch spanning between Mersey and Ribble estuaries. It is one of the largest coastal dune systems in the UK covering an area of 2100 ha and has been recognised as a nature conservation area [18]. The Sefton dune system is extremely sensitive to incoming storm waves and has experienced different morphological evolutions in the past [16,19]. Some parts of the coastline have been found to be eroding, while others are experiencing accretion, with different rates and trends. As a result, future changes in the storm climate may have significant implications on the stability and integrity of the Sefton Coast and the dune system and also may cause coastal flooding.

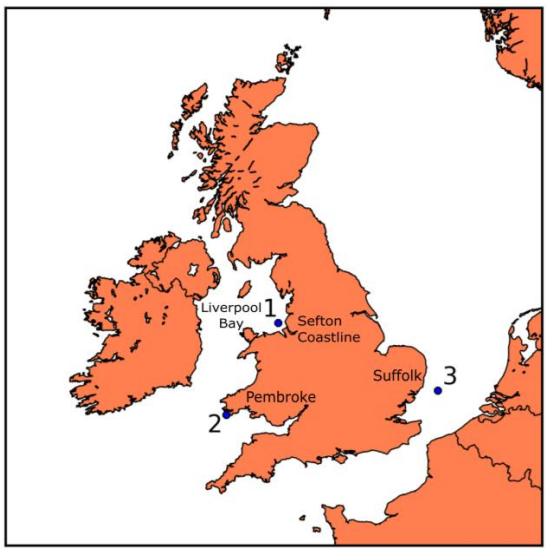

Figure 2. WaveNet buoy locations: (**1**) Liverpool Bay; (**2**) Pembroke; (**3**) West Gabbard.

2.2. Pembroke

Located approximately 4 km off the coast of Pembrokeshire in the Bristol Channel (Figure 2), in a 41-m water depth, the wave climate of Pembroke is heavily influenced by storms propagating across the Atlantic Ocean. The exposed nature of this location allows propagation of both swell and sea waves. WaveNet directional wave data are available at Pembroke from July 1998 at hourly intervals. From the measured data, the mean significant wave height was found to be 1.72 m; the maximum storm wave height was 9.4 m; and the predominant wave direction was from the southwest. Wave measurements during 1998–2009 are used for model validation in this study.

Understanding future changes to the wave climate at Pembroke is not only important for determining levels of coastal flooding and erosion for the community along the Pembrokeshire coastline, but also because Pembrokeshire has been highlighted as a potential site for tidal stream energy extraction [20,21] and wave energy harvesting [22]. Thus, any potential future changes to the incoming waves, storm climate in particular, need to be understood in order to configure and plan coastal defence and flood management, as well as marine energy extraction.

2.3. West Gabbard

The West Gabbard WaveNet buoy is located in the southern North Sea (Figure 2) in a 34-m water depth approximately 36 km off the Suffolk coastline. The wave climate in the southern North Sea has the greatest wave heights for waves approaching from the northeast and the largest fetch [23]. The predominant wave direction is south-westerly, but the wave climate also contains a north-easterly component, reflecting the wind regime [24]. Average significant wave height from the measured data was found to be 1.07 m. Most extreme events however appear to be associated with slow moving southeast tracking deeply developed low pressure systems [25]. The coastline of Suffolk has suffered from long-term cliff recession, with a rate of 3.5 m a^{-1} for the period 1883–2010 [26]. With the potential for increased storminess [9] alongside sea level rise [27] in the future, climate change is likely to result in more rapid rates of cliff retreat more frequently in the near future [26]. The WaveNet buoy at West Gabbard (Figure 2) has been operational since August 2002, providing directional wave data at 30-min intervals. Waves measured during the 2002–2009 period were used in the model validation in this study.

3. Methodology

3.1. Model Approach

The wave climate data from global wave projections [12] are described by the three-step approach detailed below.

1. A global climate simulation by an atmosphere-ocean-coupled global climate model (AOGCM) under an emission scenario.
2. A global atmospheric climate simulation with higher spatial resolution by an atmospheric global circulation model (AGCM) using sea surface temperature (SST) data from the AOGCM as a boundary condition at the bottom of AGCM.
3. A global wave simulation by a wave model forced with the sea surface winds from the AGCM.

The AGCM used in this study, developed by the Japanese Meteorological Research Institute (MRI) for IPCC AR5 [1] was MRI-AGCM3.2 [28]. The SST and perturbed physics ensemble experiments were carried out with the 60-km horizontal spatial resolution model of the MRI-AGCM3.2 (MRI-AGCM3.2H). The forcings used in the AGCM are SST, sea ice at the bottom boundary and greenhouse gases in the atmosphere.

The climate projections make use of the A1B scenario from the Special Report on Emissions Scenarios (SRES), which corresponds to Representative Concentration Pathway (RCP) 6.0 in AR5. The A1 scenario represent a more integrated world, categorised by rapid economic growth with a

population that peaks mid-21st century and then declines, where the A1B represents a balanced use of resources. The climate projections were conducted for two time slices, 1979–2009, to represent the present climate, and 2075–2099 for the future climate conditions. For the present climate, the AGCM had been forced by monthly mean observed sea ice concentration and SST from the UK Hadley centre sea ice and SST dataset [29].

Four future projection, model runs were forced by four different future SST conditions using a cluster analysis based on AOGCM projections [30]. The first SST condition (denoted as Cluster 0) is the ensemble-mean SST projected by 18 models of the Coupled Model Intercomparison Project (CMIP) 3 under the SRES A1B scenario. The other three SST conditions (Clusters 1–3) are differently classified characteristic future SST patterns derived by cluster analysis of the future change pattern of SST from 18 CMIP3 models under the A1B emission scenario. The four SSTs can objectively express the representative SSTs of the 18 CMIP3 models based on the cluster analysis. Numerous studies provide details of the atmospheric model and these scenarios [10–12].

Global wave climate projection was carried out using the WAVEWATCH III v3.14 wave model [13], forced by sea surface wind from MRI-AGCM3.2H. The global domain was set for the latitudinal range of 90 S–67 N over all longitudes with 60-km spatial grids, in order to avoid small time steps and higher computational cost incurred by the high latitude region. The directional resolution is 15°, and the frequency space is 0.04–5 Hz, which is discretised into 25 increments logarithmically as a conventional setup. It is known that mean wave height in the North Atlantic Ocean has decreasing trends and a week correlation with the NAO index [4].

3.2. Bias Correction

Due to the low resolution of the outputs from the wave model, a bias correction was applied to outputs around the UK to take into account the regional effects. The bias correction used here is the mean ratio described in Equations (1) and (2), where R is the ratio between the mean of the observed wave data ($\overline{H}_{s\ observed}$) and the mean of the modelled data ($\overline{H}_{s\ gcm}$) The corrected modelled wave heights ($H_{s\ gcm\ correcte}$) are then found by multiplying the uncorrected wave heights ($H_{s\ gcm}$) by the mean ratio R. The observed dataset used in the bias correction was limited to within the period covered by the present day model runs, 1979–2009.

$$R = \frac{\overline{H}_{s\ observed}}{\overline{H}_{s\ gcm}} \tag{1}$$

$$H_{s\ gcm\ corrected} = R \times H_{s\ gcm} \tag{2}$$

3.3. Calculation of Storm Events

This study uses a storm event definition [31] in defining storm events based on the storm wave height and the storm duration, shown in Figure 3. When the significant wave height exceeds $H_{s\ Threshold}$ for a duration (D) greater than one hour, it is classed as a storm event [32]. The threshold storm wave height ($H_{s\ Threshold}$) is estimated as 2.5 m based on the analysis of the UK Channel Coastal Observatory for Liverpool Bay [33], and considering the importance of water level as a factor for storms in Liverpool Bay. As the storm wave threshold is not defined for Pembroke and West Gabbard, it was decided to use 2.5 m as a representative threshold for all three sites. Repetition time is the duration between initial time points of two consecutive storm events (RT). The time interval (IN) between two storms provides the last time point of the previous storm and the first time point of the subsequent storms. If IN > 24 h, the second event is classed as an independent storm event. By defining storm events in this way, it allows for the investigation of changes in storm characteristics between present and future climates.

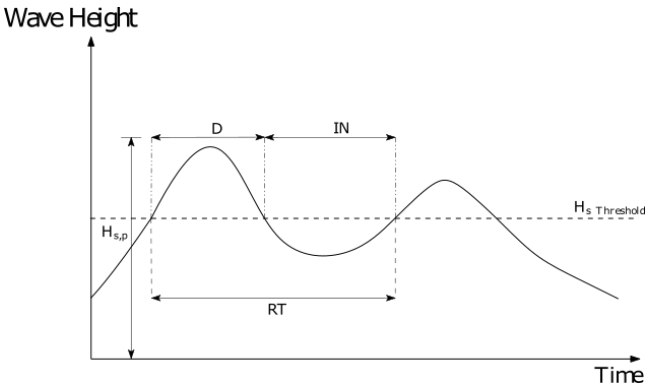

Figure 3. Storm event definition. D, duration; RT, repetition time; IN, interval.

The idea for the storm power index (S_{pi}) was first proposed in 1994 [34], finding that both storm duration and peak storm wave height play an important role in beach morphodynamic variability. Equation (3) was used to describe this relationship [35], where S_{pi} is the storm power index (in m^2h), with duration D (in hours) for which the peak storm wave height $H_{s,\,p}$ (in metres) stays above the threshold value $H_{s\ Threshold}$. In order to encompass both the storm duration and the maximum significant storm wave height in defining the strength of a storm, Equation (3) has been further modified (Equation (4)) [31]. In order to achieve more representative values for S_{pi} that are not skewed by large $H_{s,\,p}$ values, S_{pi} is now defined by the area under the storm profile shown in Figure 4, such that it is the summation given in Equation (4). In this study, Equation (4) will be used to determine storm power in order to investigate future changes in storm duration and wave height.

$$S_{pi} = D \times H_{s,p}^2 \tag{3}$$

$$S_{pi} = \sum_{i=1}^{n} \left(\Delta D \times H_i^2 \right) \tag{4}$$

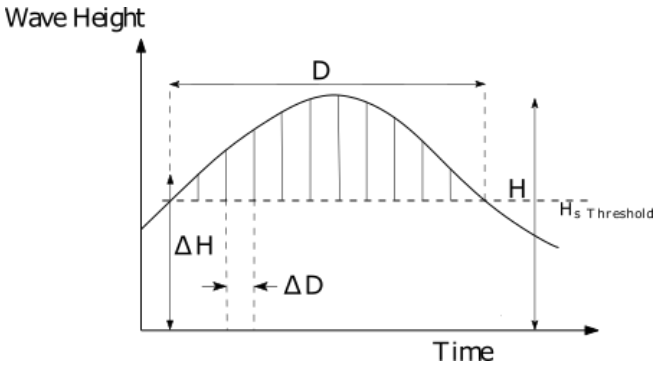

Figure 4. Schematic representation of storm power index using Equation (4) [31].

4. Results

The modelled wave data have been previously validated in the Pacific, through comparison of wind and wave fields with buoy and reanalysis data, using annual mean values [12]. The present wave projection (PWP) showed an overestimation of H_s at higher latitudes mainly attributed to the overestimation of the sea surface wind speed at 10 m (U_{10}), as well as the lack of sea ice information in the wave simulation.

As the focus here is on the storm climate in UK waters, the bias-corrected PWP data were validated against the WaveNet buoy observations at the three selected sites using statistics derived from the storm analysis of each wave dataset. The comparison of the storm climate between the PWP and the observed data was done only for the period where wave observations coincided with modelled outputs at each study site. Modelled wave outputs from the closest model grid point to the WaveNet buoy locations were selected for comparison. In order to analyse future trends of storm climate, it is advisable to use specific metrics. In this study, storm wave height (H_s), storm count and the storm power index are used in the comparisons. Trends in the future climate are then inferred by comparing the PWP climate with the future wave projection (FWP) scenarios.

Figure 5 shows the results of the comparison of annually-averaged monthly significant storm wave height and storm count at Liverpool Bay, with the error bars giving the maximum and minimum values that occurred within the record. It can be seen in Figure 5 that the wave climate at Liverpool Bay shows a winter-summer divide in terms of storm wave height and storm count. However, most storms have occurred in the winter months. The model was able to predict the variation in significant storm wave height during winter months with reasonable accuracy. However, Figure 5b, which compares modelled and measured storm count, highlights the fact that the model was not able to forecast all storms occurring during autumn and winter. The discrepancies between measured and modelled results may be largely attributed to the regional complexity of the wave climate within Liverpool Bay, alongside the coarse resolution of model outputs and also, to some extent, to the storm wave height threshold used in this study. The wave climate in Liverpool Bay is fetch limited and closely related to the local wind [36] and the complex topography. Therefore, the 60-km grid resolution may not resolve these complexities.

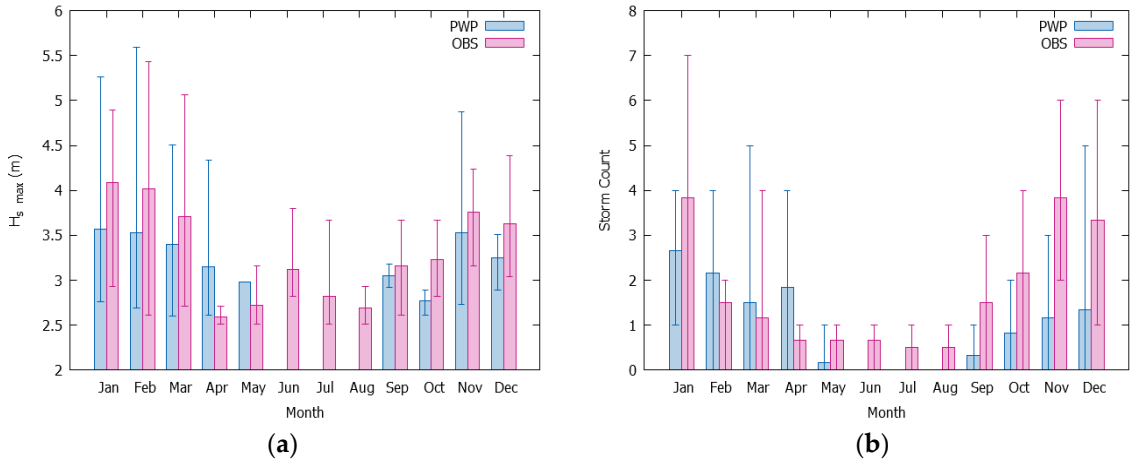

Figure 5. Comparison of observed and modelled "present" annual averaged monthly $H_{s\ max}$ and storm count for Liverpool Bay. (**a**) H_s present wave projection (PWP) compared to the observed (OBS); (**b**) storm count PWP compared to the observed.

The comparison of modelled and measured storms at Pembroke is shown in Figure 6. The model performance at this site is in very good agreement with the measured storm data, which would be expected due to the exposed nature of the site where the wave climate is less influenced by regional effects and is more closely linked to the North Atlantic Ocean. It should also be noted that although the storm wave heights in Pembroke show a clear difference between summer and winter months, the difference between the numbers of storms occurring in winter and summer months is less obvious. This may well be attributed to the selection of the storm threshold.

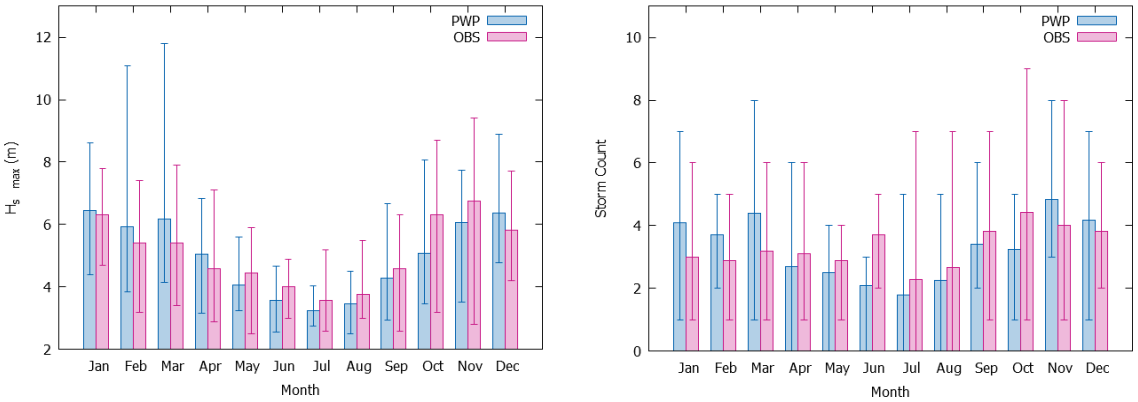

Figure 6. Comparison of the observed and modelled "present" annual averaged monthly $H_{s\ \max}$ and storm count for Pembroke. (**a**) H_s PWP compared to the observed; (**b**) storm count PWP compared to the observed.

In Figure 7, the comparison of observed and modelled storm waves at the West Gabbard site is shown. Figure 7a shows good agreement between observed and modelled annual averaged monthly storm wave heights. It also highlights that the seasonality of storm wave height at this location is less obvious. There is however a strong seasonal variation in storm count that can be seen. Modelled and measured storm wave height and storm count show very good agreement at this site. The location of the West Gabbard buoy, in comparatively deep water, which is less influenced by regional effects and complex conditions, may have contributed to the very encouraging comparisons.

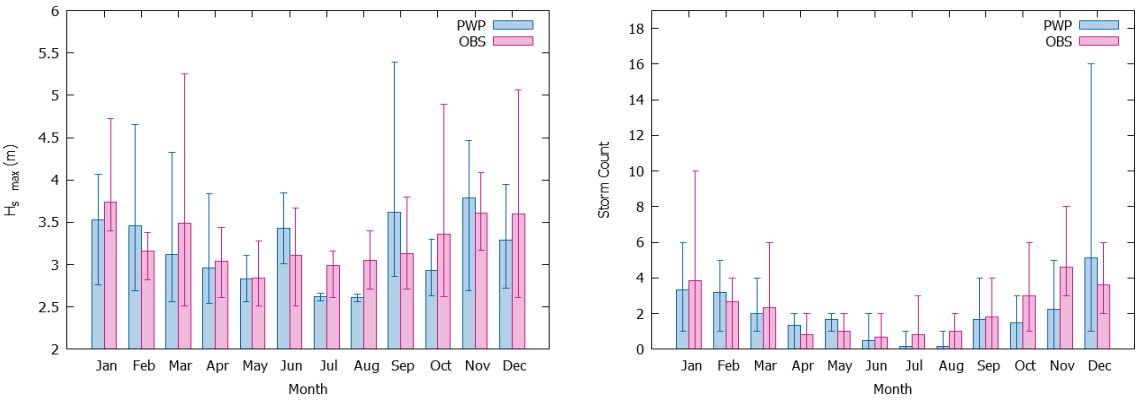

Figure 7. Comparison of observed and modelled "present" annual averaged monthly $H_{s\ \max}$ and storm count for West Gabbard. (**a**) H_s PWP compared to the observed; (**b**) storm count PWP compared to the observed.

The above comparisons of storm climates at three distinctly-different sites around the UK reveal that the wave model was able to forecast storm conditions at sites that are not significantly influenced by local/regional complexities. Therefore, the globally-predicted wave data can be used to investigate climate change impacts on the UK storm climate, at locations that are not locally affected, with reasonable confidence. As such, only Pembroke and West Gabbard future storm climates are investigated in the following section.

5. Results and Discussion

In this section, future storm climate at Pembroke and West Gabbard, modelled under a cluster of Scenarios C0, C1, C2 and C3, was analysed, where C0 represents the ensemble mean of the A1B scenario, and the other three clusters are differently classified future SST patterns from 18 CMIP3 models under the A1B emission scenario [30]. The results are then compared with the "present" (PWP) storm climate. Changes in future storm climate are inferred through the comparison of the averaged monthly statistics of modelled data for the present climate and for the future climate scenarios. Ensemble mean and maximum differences are expressed in Equations (5) and (6), respectively.

$$\text{Ensemble mean difference} = \sum_{i=0}^{3} \left(FWP\ Ci - PWP\right)/4 \tag{5}$$

$$\text{Ensemble}\underset{i=0,1,2,3}{\text{maximum difference}} = \max\left(FWP\ Ci - PWP\right) - \min\left(FWP\ Ci - PWP\right) \tag{6}$$

5.1. Pembroke

Figure 8 shows the average monthly peak significant storm wave height ($H_{s\ \max}$), averaged over the period from 2075–2099 for the four future scenarios for Pembroke. The similar result for the "present" (PWP) scenario is also shown. There is no apparent overall difference between $H_{s\ \max}$ in "present" and "future" conditions. Furthermore, there is no clear and consistent trend in the change in storm wave height within the four future scenarios; the different conditions show variability, which is close to the PWP value, but also not consistent within all of the scenarios: some months show both decreasing and increasing storm wave height with respect to the PWP. It can be seen in this figure that a very clear seasonal signature exists in peak storm wave height, similar to that in the PWP scenario, with higher average peak storm wave heights occurring throughout the winter months compared with summer months. The winter months also show a higher variation in average $H_{s\ \max}$ than the summer months; for example, clusters C1 and C3 show approximately a 12% increase from the PWP in January, with C1 also giving a 17% increase in February. November and December also display large deviations from PWP, with C3 giving a 14% increase in November and C1 and C2 giving 10% and 11% increases in December, respectively. May shows the largest variation of average $H_{s\ \max}$ around the PWP with approximately a 23% difference between the C3 and C2 with respect to the PWP. The C3 scenario shows the most consistent change from the PWP, with a total of nine months displaying a difference greater than 5%. C0, however, representing the ensemble mean of A1B, only shows a difference greater than 5% in four months, with only one greater than 10%, indicating little change in future storm wave height when all model groups are accounted for. Table 1 displays the average PWP values from Figure 8 with the differences between each future cluster average and the PWP (ΔAvg), as well as the standard deviation and ensemble mean difference and ensemble maximum difference. The variation within the projections, and seasonally, is highlighted, with the ensemble maximum difference greater than 0.7 m in six months. With the ensemble mean difference taking all projections in to account, the inconsistent trend previously described is clearly shown, although the mean difference is slightly large across the winter compared to summer.

Table 1. Pembroke comparison of present (PWP) and future (FWP-C0–C3) $H_{s\ max}$.

Month	PWP (m)		FWP C0 (m)		FWP C1 (m)		FWP C2 (m)		FWP C3 (m)		Ensemble Mean Difference (m)	Ensemble Maximum Difference (m)
	Avg	SD	ΔAvg	SD	ΔAvg	SD	ΔAvg	SD	ΔAvg	SD		
January	6.58	1.53	−0.01	1.71	0.76	2.12	0.26	1.43	0.79	2.07	0.45	0.80
February	5.63	1.80	−0.02	1.24	0.97	1.58	0.36	1.42	0.33	1.51	0.41	0.99
March	5.60	1.64	0.61	1.77	0.21	1.82	0.00	1.19	−0.12	1.48	0.18	0.73
April	4.96	1.57	−0.04	1.49	−0.12	1.17	−0.03	1.11	−0.52	1.01	−0.17	0.49
May	4.27	1.47	−0.25	1.40	−0.08	0.90	−0.50	1.41	0.50	1.89	−0.08	1.00
June	3.49	1.38	0.19	1.78	0.09	1.87	0.12	1.64	−0.13	1.62	0.07	0.32
July	3.27	1.06	−0.03	1.68	0.19	1.82	0.10	1.75	−0.27	1.57	0.00	0.46
August	3.27	1.55	0.03	1.55	0.17	1.67	0.29	1.86	0.30	1.65	0.20	0.27
September	4.23	1.21	−0.15	1.41	−0.17	1.13	−0.13	1.54	−0.30	1.35	−0.19	0.17
October	4.90	1.44	0.23	1.00	0.00	0.93	0.15	0.94	0.26	1.65	0.16	0.26
November	5.88	1.76	0.08	1.70	−0.03	1.94	0.28	1.18	0.80	1.69	0.28	0.83
December	6.46	1.23	−0.10	1.14	0.68	1.86	0.75	1.72	–0.31	1.70	0.25	1.06

Avg—Average, SD—Standard Deviation, ΔAvg—Difference between future cluster average and the PWP average.

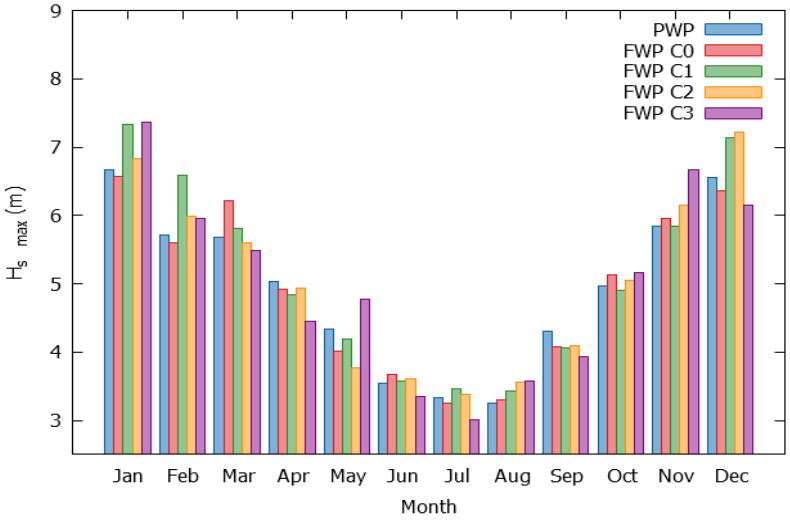

Figure 8. Comparison of the present (PWP) and future (FWP, clusters C0–C3) averaged monthly maximum storm wave height $H_{s\ \max}$ at Pembroke.

In Figure 9, the average monthly storm counts at Pembroke for the PWP and future scenarios are shown. The results show an indication of a potential change in storm count due to climate change. There is a clear trend of seasonality, with fewer storms occurring in the summer months and more storms occurring during winter months excluding December, displayed across all of the scenarios. However, a significant variability is seen between different future scenarios (C0–C3). December shows a range of variability greater than 10% from the PWP average: the largest variability is in July, where all scenarios show a reduction in average storm count. C3 scenario gives 65% fewer storms than the current PWP scenario in July. All scenarios show a reduction in storm count across the months April–September, apart from the 20% and 8% increases shown by C0 and C2 in June and the 13% increase in May in the C3 scenario. Through October–March, there are increases in storm count in the range up to 30% and 17% in October and November respectively, small reductions in December up to 7%, and then up to 23% in January, followed by increases in February and March between 3% (C1) and 13% (C2 and C0) and 1% (C3) and 16% (C2). As seen in Figure 8, the highest variation of $H_{s\ \max}$ is shown in the C3 scenario, with an average difference of 8% across all months, compared to 5%, 5.5% and 3% in C2, C1 and C0, respectively. However, in Figure 9, all four scenarios show similar average variation of storm count between 14% for C0 and 15.5% for C3.

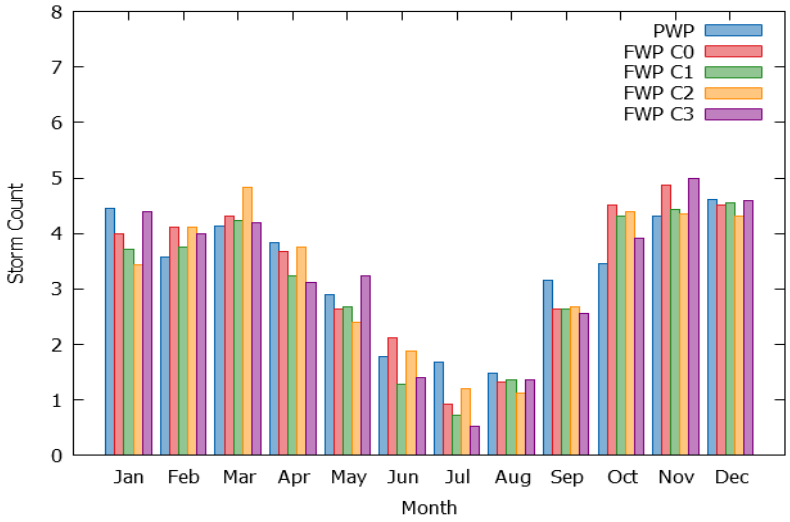

Figure 9. Comparison of present (PWP) and future (FWP-C0–C3) storm count at Pembroke.

Figure 10 shows the average monthly cumulative storm comparison of present (PWP) and future (FWP-C0–C3) storm count at the Pembroke power index S_{pi} (Equation (4)). Similarly to $H_{s\ \max}$, S_{pi} shows a large seasonal variation. This can partly be attributed to Equation (4), which uses $H_{s\ \max}$; however, there are also potentially higher duration storms occurring during the winter months in comparison to the summer months. All C0–C3 scenarios show similar trends. The highest percentage variation between the four scenarios and PWP is observed across the summer months, April–September, and is linked to changes in the number of storms in Figure 9 and wave height in Figure 8. Most months and scenario combinations show a decrease in line with the changes in storm count, giving reductions up to 64% and the level of change between 35% and 61%. However, the increases in storm count for C0 and C2 in June are also observed in the storm power, with increases of 45% and 37%, respectively, and also a 20% increase in C3 in May. The 20% increase of C3 in May can potentially be linked to the 12% in wave height, but these interactions demonstrate the complexity in understanding future changes in storm climate. Despite the high percentage variation across the summer months, the relative difference across the winter months is noticeable and of great importance. Due to the magnitude of storm power, these changes could increase the risk of coastal flooding and storm-driven beach erosion. October–March show a rise in storm powers in the majority of clusters with the exception of an 11% decrease in C3 in December and 2% decreases in C2 in February and C0 in December. As with Figures 8 and 9, the largest changes are observed with C3, but the general trend towards increases in winter and decreases in summer is observed across all scenarios.

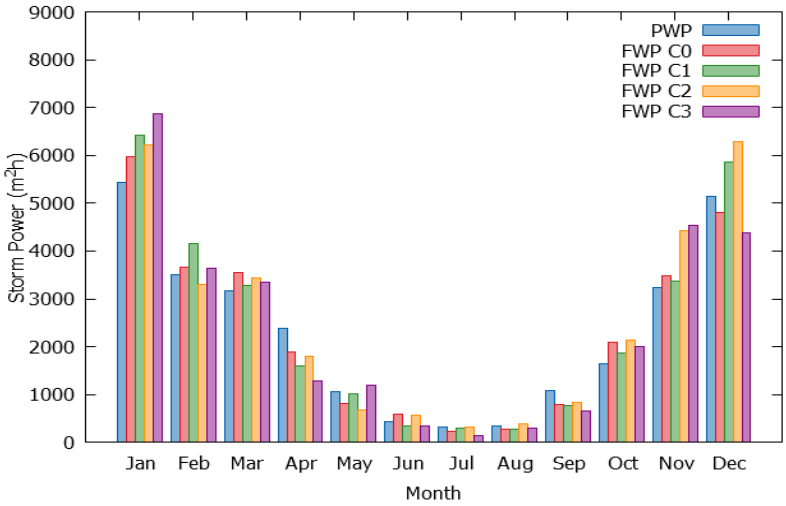

Figure 10. Comparison of present (PWP) and future (FWP-C0–C3) storm power index (S_{pi}) at Pembroke.

5.2. West Gabbard

A comparison of average monthly peak storm wave height for present (PWP) and future (FWP) climate scenarios in West Gabbard is shown in Figure 11. All future clusters show some seasonal variability of $H_{s\ \max}$; however, storm wave height variability between clusters is considerable. For example, the monthly average $H_{s\ \max}$ for C3 is less than PWP for seven months, but that for C1 is higher than PWP for 10 months. November and June are the only two months with clear differences from the PWP with all clusters displaying a similar decisive trend; with all clusters giving a greater than 5% increase in $H_{s\ \max}$ in November and giving a greater than 4% reduction in June. March, August, September and October, however, also show consistent changes with all clusters, but due to their magnitude, it is difficult to attribute a clear trend. The C0 results give increased $H_{s\ \max}$ in seven months with no trend of seasonality. As with Table 1 for Pembroke, Table 2 presents the variation in peak storm wave height at West Gabbard. The small magnitude changes in $H_{s\ \max}$ are also shown in the ensemble mean difference; taking in to account all scenarios gives an inconsistent picture. However, due these low values and the inconsistent pattern in changes, the results suggest that there is little change in future $H_{s\ \max}$ at West Gabbard.

Table 2. West Gabbard comparison of present (PWP) and future (FWP-C0–C3) $H_{s\ \max}$.

Month	PWP (m)		FWP C0 (m)		FWP C1 (m)		FWP C2 (m)		FWP C3 (m)		Ensemble Mean Difference (m)	Ensemble Maximum Difference (m)
	Avg	SD	ΔAvg	SD	ΔAvg	SD	ΔAvg	SD	ΔAvg	SD		
January	3.84	1.15	0.23	0.86	0.07	1.15	0.12	0.62	0.65	1.11	0.27	0.58
February	3.69	1.51	−0.02	1.34	0.33	1.32	0.32	1.08	−0.20	1.29	0.11	0.53
March	3.37	1.25	0.04	0.95	0.14	0.95	0.04	1.08	0.06	1.61	0.07	0.10
April	3.16	1.32	0.11	1.36	0.10	1.48	0.07	1.64	−0.12	1.59	0.04	0.23
May	3.07	1.53	0.04	1.61	0.05	1.58	0.14	1.65	−0.05	1.55	0.04	0.19
June	3.09	1.51	−0.25	1.46	−0.33	1.36	−0.11	1.40	−0.31	1.37	−0.25	0.22
July	2.82	1.32	−0.06	1.04	0.16	0.99	0.01	1.30	−0.11	1.02	0.00	0.27
August	2.69	1.19	0.31	1.16	0.38	1.35	0.11	1.05	0.04	1.30	0.21	0.34
September	3.28	1.67	−0.17	1.67	−0.19	1.55	−0.24	1.56	−0.01	1.86	−0.15	0.23
October	3.10	1.14	0.06	1.36	0.03	1.31	0.28	1.34	0.15	1.45	0.13	0.25
November	3.39	1.37	0.32	1.60	0.21	1.61	0.24	0.89	0.23	0.92	0.25	0.11
December	4.03	0.89	−0.38	0.75	0.27	1.48	−0.24	1.31	−0.30	1.23	−0.16	0.66

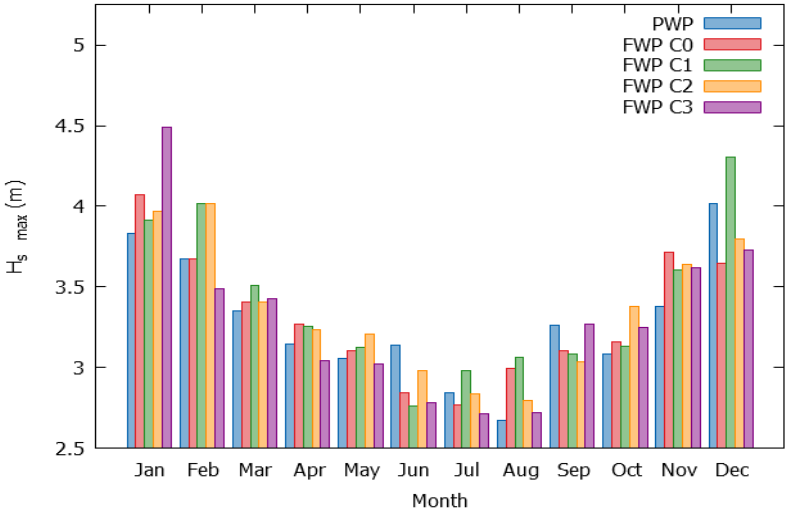

Figure 11. Comparison of present (PWP) and future (FWP-C0–C3) averaged monthly maximum storm wave height $H_{s\ \max}$ at West Gabbard.

The average monthly present and future storm count for West Gabbard is shown in Figure 12. The average monthly storm count shows greater seasonal variation than the storm wave height. In future C1, C2 and C3 clusters, the storm count is reduced when compared to present PWP throughout the period February–September, with the exception of C1 in February giving a 2% increase, C2 in July giving a 1.5% increase and C3 in August giving a 10% increase. C0 shows a more mixed trend across this period, where storm count is larger than PWP for six months and smaller than PWP for six months. The overall change in storm count between PWP and future scenarios is not clear. Winter months, October, November and January, show a future increase in storm count across all clusters, with December giving a mixture of increase and decreases. Throughout the majority of months, C1, C2 and C3 tend to show slight changes from the PWP data, highlighting the potential extremities in the A1B scenario. C0 does however show an overall decrease in storm count when compared to PWP, with the largest increase occurring in October (21%). With C0 representing the ensemble mean of the A1B scenario and C1, C2 and C3 representing different model groups, while also displaying a similar but more extreme trend as C0, these results suggest a reduction in the frequency of storms across the summer and a potential increase in the winter in West Gabbard.

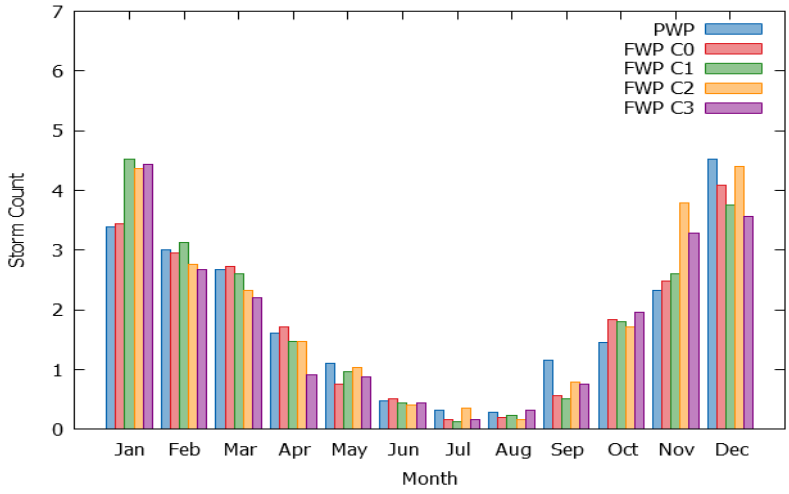

Figure 12. Comparison of present (PWP) and future (FWP-C0–C3) storm count at West Gabbard.

Finally, Figure 13 shows the average monthly cumulative storm power index results for the PWP and four future clusters at West Gabbard. It is clear that West Gabbard suffers from a less intense storm climate than that of Pembroke (Figure 10), as it is located in the North Sea with a smaller fetch. Figure 13 reveals that there is a tendency of decreases in the storm power in the future across the summer months, mainly during the period from April–September. This may be due to the decrease in storm count, which would reduce the cumulative storm duration within a given month and, hence, the storm power. Through the period from April–September, in May, June, July and September, all future clusters show consistent reductions in storm power, except C2 giving a 13% increase and C0 giving a 5% increase in April. In August, however, C1 gives a much larger variation of storm power, with C1, C2 and C3 increasing by 91%, 34% and 40%, respectively, and C0 decreasing by 18%. The storm power is consistently larger in the future when compared to PWP throughout the winter months, with only a few exceptions in January. As with Section 5.1, C1, C2 and C3 give higher variability from PWP than C0. However, C0 gives an 18% increase in March, a 34% increase in October and a 27% increase in November.

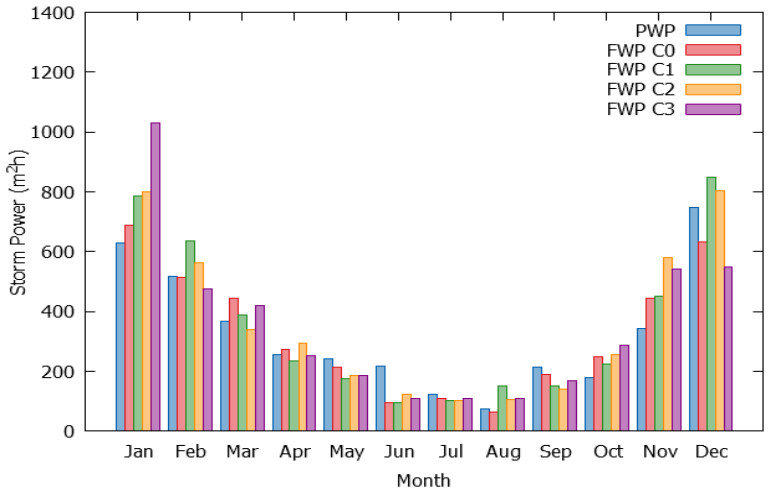

Figure 13. Comparison of present (PWP) and future (FWP-C0–C3) storm power index (S_{pi}) at West Gabbard.

6. Summary and Conclusions

Future projections of global and UK climate have been carried out using the MRI-AGCM3.2H atmospheric global climate model and the WAVEWATCH III wave model. In order to investigate future changes in the UK storm climate, proxy conditions of maximum significant storm wave height, storm duration, storm count and storm power index were used to investigate potential changes. Three sites around the UK that represent a variety of different site conditions, where long-term measured wave data are available for a reasonable length of time, are chosen for this study. First, the model outputs for the present climate scenario (PWP) were examined and compared with observed storm data using the chosen proxy conditions in order to validate the models' performance and investigate the reliability of future projections. The comparison of modelled PWP scenario-derived results at West Gabbard and Pembroke showed that the model correctly reproduced the current storm climate at both sites very satisfactorily. The model did not capture the storm conditions at Liverpool Bay very well; however, considering the complex local and regional setting at this site, this should be expected.

Following the validation of model outputs, it was chosen to investigate future changes of the storm climate only at Pembroke and West Gabbard. The results of the four different future cluster scenarios (FWP-C0, C1, C2, C3) were compared with the PWP dataset to investigate future changes in storm climate, using the same proxy conditions used for model-data comparison. While there were no clear and consistent trends across all clusters, monthly and seasonal changes in the storm wave climate were observed at both sites.

FWP C0, representing the ensemble mean for A1B, had the lowest overall variability compared to the PWP, with C1, C2 and C3 showing increased variation. However, ensemble changes in storm characteristics, when compared with their inherent variation and considering the impact of existing teleconnections, such as the NAO, were small. As winter storms are significantly correlated with NAO [37], it is important to take account of their effects when investigating future characteristics. In an analysis of the UK Climate Projections (UKCP) 09 [9] findings, it was found that it was unlikely that a statistically-significant change in storminess would occur in Liverpool Bay between 1960 and 2100 [16], similar to the results of this study. However, in an analysis of wave climate changes in the Western North Pacific [12], it was shown that changes in tropical cyclone behaviour influenced the summertime wave height and therefore being sensitive to SST. This reinforces the need for regional investigations due to the complex local relations. Since this study only uses forcing within the A1B scenario, it does not represent the full range of potential variation in storm wave climate due to future climate change. Insights in to future changes in UK storm wave climate are important. Their potential impacts on flood risk and coastal management should continue to be investigated, incorporating regional downscaling, to allow for informed decision making.

Acknowledgments: W.G.B. acknowledges the support of EPSRC-DTA funds to pursue his PhD studies at Swansea University. H.K. acknowledges the support of the EPSRC funded FloodMEMORY (EP/K013513/1) project for providing some data used in this study. H.K. and D.E.R. acknowledge the support of the British Council funded Ensemble Estimation of Flood Risk in a Changing Climate project. P. Dissanayake at University of Konstanz, Germany, is appreciated for the support provided during the preliminary data analysis. Finally, the Cente for Environment, Fisheries and Aquaculture Science (CEFAS) is acknowledged for providing wave data (WaveNet).

Author Contributions: W.G.B., H.K., D.R. and N.M. conceived of the process for analysis. W.G.B., H.K. and D.R. analysed the data. N.M. contributed the datasets and provided advice on the analysis. W.G.B. wrote the paper.

Conflicts of Interest: The authors declare no conflict of interest.

References

1. IPCC. *Climate Change 2013: The Physical Science Basis. Contribution of Working Group I to the Fifth Assessment Report of the Intergovernmental Panel on Climate Change*; Cambridge University Press: Cambridge, UK, 2013.
2. Semedo, A.; Weisse, R.; Behrens, A.; Sterl, A.; Bengtsson, L.; Gunther, H. Projection of Global Wave Climate Change toward the End of the Twenty-First Century. *J. Clim.* **2013**, *26*, 8269–8288. [CrossRef]
3. Hemer, M.; Wang, X.L.; Weisse, R.; Swail, V.R. Advancing wind-waves climate science: The COWCLIP project. *Bull. Am. Meteorol. Soc.* **2012**, *93*, 791–796. [CrossRef]
4. Hemer, M.; Fan, Y.; Mori, N.; Semedo, A.; Wang, X.L. Projected changes in wave climate from a multi-model ensemble. *Nat. Clim. Chang.* **2013**, *3*, 471–476. [CrossRef]
5. IPCC. *Climate Change 2007: Impacts, Adaptation and Vulnerability. Contribution of Working Group II to the Fourth Assessment Report of the Intergovernmental Panel on Climate Change*; Cambridge University Press: Cambridge, UK, 2007.
6. Grabemann, I.; Weisse, R. Climate change impact on extreme wave conditions in the North Sea: An ensemble study. *Ocean Dyn.* **2008**, *58*, 199–212. [CrossRef]
7. Debernard, J.B.; Røed, L.P. Future wind, wave and storm surge climate in the Northern Seas: A revisit. *Tellus A* **2008**, *60*, 427–438. [CrossRef]
8. Zacharioudaki, A.; Pan, S.; Simmonds, D.; Magar, V.; Reeve, D.E. Future wave climate over the west-European shelf seas. *Ocean Dyn.* **2011**, *61*, 807–827. [CrossRef]
9. Lowe, J.A.; Howard, T.P.; Pardaens, A.; Tinker, J.; Holt, J.; Wakelin, S.; Milne, G.; Leake, J.; Wolf, J.; Horsburgh, K.; et al. *UK Climate Projections Science Report: Marine and Coastal Projections*; Technnical Report; Met Office Hadley Centre: Exeter, UK, 2009.
10. Mori, N.; Yasuda, T.; Mase, H.; Tom, T.; Oku, Y. Projection of Extreme Wave Climate Change under Global Warming. *Hydrol. Res. Lett.* **2010**, *71*, 122–129. [CrossRef]
11. Mori, N.; Shimura, T.; Yasuda, T.; Mase, H. Multi-model climate projections of ocean surface variables under different climate scenarios Future change of waves, sea level and wind. *Ocean Eng.* **2013**, *4*, 15–19. [CrossRef]
12. Shimura, T.; Mori, N.; Mase, H. Future Projection of Ocean Wave Climate: Analysis of SST Impacts on Wave Climate Changes in the Western North Pacific. *J. Clim.* **2015**, *28*, 3171–3190. [CrossRef]

13. Tolman, H.L. *User Manual and System Documentation of WAVEWATCH III^{TM} Version 3.14*; Technical Note; NOAA/NWS/NCEP/MMAB: College Park, MD, USA, 2009.
14. Plater, A.J.; Grenville, J. Liverpool bay: Linking the eastern Irish Sea to the Sefton coast. In *Sefton's Dynamic Coast, Proceedings of the Conference on Coastal Geomorphology, Biogeography and Management*, 1st ed.; Worsley, A.T., Lymbery, G., Holden, V.J.C., Newton, M., Eds.; 2008; pp. 28–54.
15. Brown, J.M.; Wolf, J.; Souza, A.J. Past to future extreme events in Liverpool Bay: Model projections from 1960–2100. *Clim. Chang.* **2011**, *111*, 365–391. [CrossRef]
16. Esteves, L.S.; Williams, J.J.; Brown, J.M. Looking for evidence of climate change impacts in the eastern Irish Sea. *Nat. Hazards Earth Syst. Sci.* **2011**, *11*, 1641–1656. [CrossRef]
17. Brown, J.M.; Souza, A.J.; Wolf, J. An 11-year validation of wave-surge modelling in the Irish Sea, using a nested POLCOMSWAM modelling system. *Ocean Model.* **2010**, *33*, 118–128. [CrossRef]
18. Esteves, L.S.; Brown, J.M.; Williams, J.J.; Lymbery, G. Quantifying thresholds for significant dune erosion along the Sefton Coast, Northwest England. *Geomorphology* **2012**, *143–144*, 52–61. [CrossRef]
19. Pye, K.; Blott, S. Decadal-scale variation in dune erosion and accretion rates: An investigation of the significance of changing storm tide frequency and magnitude on the Sefton coast, UK. *Geomorphology* **2008**, *102*, 652–666. [CrossRef]
20. Fairley, I.; Neill, S.; Wrobelowski, T.; Willis, M.; Masters, I. Potential Array Sites for Tidal Stream Electricity Generation off the Pembrokeshire Coast. In Proceedings of the 9th European Wave and Tidal Energy Conference (EWTEC), Southampton, UK, 5–9 September 2011.
21. Fairley, I.; Evans, P.; Wooldridge, C.; Willis, M.; Masters, I. Evaluation of tidal stream resource in a potential array area via direct measurements. *Renew. Energy* **2013**, *57*, 70–78. [CrossRef]
22. Bento, A.R.; Martinho, P.; Guedes Soares, C.; Bento, A.R.; Martinho, P.; Guedes Soares, C. Modelling wave energy resources for UK's southwest coast. In Proceedings of the IEEE Oceans Conference, Santander, Spain, 6–9 June 2013.
23. Carr, A. Sizewell-dunwich banks field study. In *Topic Report: 2. Long-Term Changes in the Coastline and Offshore Banks: Report No.89*; Technical Report; Institute of Oceanographic Sciences: Taunton, UK, 1979.
24. Brooks, S.M. *Coastal Change in Historic Times—Linking Offshore Bathymetry Changes and Cliff Recession in Suffolk*; Technical Report; The Crown Estate: London, UK, 2010.
25. Muir Wood, R.; Drayton, M.; Berger, A.; Burgess, P.; Wright, T. Catastrophe loss modelling of storm-surge flood risk in eastern England. *Philos. Trans. A Math. Phys. Eng. Sci.* **2005**, *363*, 1407–1422. [CrossRef] [PubMed]
26. Brooks, S.; Spencer, T.; Boreham, S. Deriving mechanisms and thresholds for cliff retreat in soft-rock cliffs under changing climates: Rapidly retreating cliffs of the Suffolk coast, U.K. *Geomorphology* **2012**, *153–154*, 48–60. [CrossRef]
27. Church, J.A.; White, N.J. A 20th century acceleration in global sea-level rise. *Geophys. Res. Lett.* **2006**, *33*. [CrossRef]
28. Mizuta, R.; Yoshimura, H.; Murakami, H.; Matsueda, M.; Endo, H.; Ose, T.; Kamiguchi, K.; Hosaka, M.; Sugi, M.; Yukimoto, S.; et al. Climate Simulations Using MRI-AGCM3.2 with 20-km Grid. *J. Meteorol. Soc. Jpn.* **2012**, *90A*, 238–258. [CrossRef]
29. Rayner, N.; Parker, D.; Horton, E.; Folland, C.; Alexander, L.; Rowell, D.; Kent, E.; Kaplan, A. Global analyses of sea surface temperature, sea ice, and night marine air temperature since the late Nineteenth Century. *J. Geophys. Res.* **2003**, *108*. [CrossRef]
30. Murakami, H.; Mizuta, R.; Shindo, E. Future changes in tropical cyclone activity projected by multi-physics and multi-SST ensemble experiments using the 60-km-mesh MRI-AGCM. *Clim. Dyn.* **2012**, *39*, 2569–2584. [CrossRef]
31. Dissanayake, P.; Brown, J.; Wisse, P.; Karunarathna, H. Comparison of storm cluster vs isolated event impacts on beach/dune morphodynamics. *Estuar. Coast. Shelf Sci.* **2015**, *164*, 301–312. [CrossRef]
32. Callaghan, D.; Nielsen, P.; Short, A.; Ranasinghe, R. Comparison of storm cluster vs isolated event impacts on beach/dune morphodynamics. *Coast. Eng.* **2008**, *55*, 375–390. [CrossRef]
33. Coastal Engineering UK Ltd. *Sefton Council Strategic Annual Coastal Performance Review 2010*; Technical note; Sefton Council: Southport, UK, 2011.
34. Dolan, R.; Davies, R. Coastal storm hazards. *J. Coast. Res.* **1994**, *12*, 103–114.

35. Karunarathna, H.; Pender, D.; Ranasinghe, R.; Short, A.D.; Reeve, D.E. The effects of storm clustering on beach profile variability. *Mar. Geol.* **2014**, *348*, 103–112. [CrossRef]
36. Wolf, J.; Brown, J.M.; Howarth, M.J. The wave climate of Liverpool Bay observations and modelling. *Ocean Dyn.* **2011**, *61*, 639–655. [CrossRef]
37. Allan, R.; Tett, S.; Alexander, L. Fluctuations in autumn-winter severe storms over the British Isles: 1920 to present. *Int. J. Climatol.* **2009**, *29*, 357–371. [CrossRef]